Pressure-induced yttrium oxides with unconventional stoichiometries and novel properties

Qiuping Yang [1,2,*] Jianyan Lin,[2,3,*] Fei Li,[1,2] Jing Zhang,[2] Eva Zurek [4,†] and Guochun Yang [1,2,‡]

[1]*State Key Laboratory of Metastable Materials Science & Technology and Key Laboratory for Microstructural Material Physics of Hebei Province, School of Science, Yanshan University, Qinhuangdao 066004, China*

[2]*Centre for Advanced Optoelectronic Functional Materials Research and Key Laboratory for UV Light-Emitting Materials and Technology of Ministry of Education, Northeast Normal University, Changchun 130024, China*

[3]*College of Physics, Changchun Normal University, Changchun 130032, China*

[4]*Department of Chemistry, State University of New York at Buffalo, Buffalo, New York 14260, USA*

(Received 26 January 2021; accepted 29 March 2021; published 9 April 2021)

The oxygenic motifs (e.g., O^{2-}, O_2^{2-} O_2^{2-}, and O_2^{-}) that are present in compounds have a substantial effect on their electronic structure and behavior. Herein, first-principles swarm-intelligence crystal structural searches reveal that the reaction between Y and O under high pressure leads to the formation of novel compounds with unique properties. Several O-rich Y-O compounds (e.g., YO_2, Y_2O_5, and YO_3) emerge as being stable. It is shown that the oxygenic motifs found within the stable species depend upon the oxygen content and pressure (e.g., O^{2-} in YO and Y_2O_3, the coexistence of O^{2-} and O_2^{2-} in YO_2 and Y_2O_5, O_2^{2-} in *Pm*-3 YO_3, and O^{2-} in *Cmcm* YO_3), and are accompanied by a transition in the electronic structure from superconducting to metallic to semiconducting. Notably, the *Cmcm* symmetry YO_3 phase, consisting of a 13-fold coordinated face-sharing polyhedron with 15 faces, can be classified as a transition metal (TM) superoxide. The long sought-after bulk yttrium monoxide (YO) is shown to become stable at high pressure. NaCl-type YO is superconducting with a critical temperature (T_c) of 13.0 K at 25 GPa, becoming the TM monoxide with the highest known T_c. Our work will inspire future studies exploring the chemistry and properties of O-rich TM oxides at high pressure.

DOI: 10.1103/PhysRevMaterials.5.044802

I. INTRODUCTION

The discovery of new types of superconducting materials and development of a microscopic understanding of the mechanism of superconductivity are important and challenging tasks in condensed matter physics and chemistry [1,2]. Much research has been directed to high-pressure hydrides [3], and copper/iron-based materials [4]. Several theoretical studies have suggested promising candidates, and experiments have synthesized materials that have approached [5,6], and recently achieved the dream of room-temperature superconductivity [7]. The superconducting mechanism may be conventional electron-phonon mediated or unconventional. The former can be understood within the framework of Bardeen-Cooper-Schrieffer theory, making it possible to theoretically design superconductors [8].

Transition metal (TM) atoms have diverse *d* electron configurations, resulting in a wide range of potential compounds they can form with other elements [9]. The *d*-orbital occupation numbers assumed in compounds are not only associated with the valence state of the TM atoms, but are also important for their structure and properties [10–12]. For example, IrF_8 with a $5d^1$ electron configuration is metallic, while OsF_8 with a $5d^\circ$ configuration is semiconducting. The oxidating ability of IrF_8 is stronger than OsF_8 [13,14]. Thus, developing strategies to manipulate the *d*-orbital electron count within TM atoms in compounds is of fundamental interest to advance materials science [15].

Oxygen is a charming element. Most of its compounds are semiconductors and form ionic compounds because oxygen is a strong oxidizing agent. The eighth element can assume a variety of motifs (e.g., O^{2-}, O_2^{2-}, O^{2-}, and O_3^{2-}) within compounds, exhibiting different oxidation states (e.g., –2, –1, and –0.5), which can play a key role in its physical/chemical properties. Li_2O_2 with O_2^{2-} (peroxide) is insulating, LiO_2 comprised of O^{2-} (superoxide) is paramagnetic, whereas Li_3O_4, containing both O_2^{2-} and O^{2-}, exhibits intriguing half-metallic magnetism [16]. Therefore, exploring the forms oxygen adopts within compounds has drawn great attention. O_2^{2-} and O^{2-} often appear in main-group metal oxides, however, only a few TM oxides (e.g., FeO_2 [17], Ti_2O_5 [18], HfO_3 [19], ZrO_3 [20], and VO_4 [21]) containing O^{2-} and/or O_2^{2-} anions have been reported. To the best of our knowledge, no TM superoxide is known thus far.

Pressure has become an irreplaceable tool in synthesizing new materials that are not accessible at atmospheric conditions [22]. It is also beneficial for inducing metallization and superconductivity in compounds [23]. The properties of materials are strongly correlated with their chemical compositions [24]. Experiments and first-principles calculations have shown that pressure can lead to the formation of a

*These authors contributed equally to this work.
†Corresponding author: ezurek@buffalo.edu
‡Corresponding author: yanggc468@nenu.edu.cn

plethora of compounds with unusual stoichiometries and exotic properties [25]. For example, TiO_2 is a semiconductor and a multifunctional material (e.g., pigment, capacitor, memory device, and photocatalyst) at ambient conditions, whereas thin films of TiO, Ti_3O_5, and Ti_4O_7 are metallic and superconducting [26]. Under compression, several stoichiometric Ti-rich Ti_4O and Ti_5O [27], as well as O-rich Ti_2O_5 and TiO_3 [18] phases have been predicted, with electride and peroxide character, respectively. For the V-O system, two stoichiometric V_2O and VO_4 phases have been predicted to become stable at high pressures. Interestingly, V_2O is computed to be superconducting, becoming an example of a conventional superconductor in the V-O system, while VO_4, containing O^{2-} and $O_2{}^{2-}$, shows semiconducting behavior with the unusual phenomenon of pressure-induced band gap increase [21].

Yttrium (Y), has a $3d^14s^2$ electron configuration and can assume +1, +2 or +3 oxidation states. At ambient conditions its only stable oxide is Y_2O_3, in which Y has an oxidation state of +3 [28]. Much attention has been paid to Y_2O_3 due to its high stability, excellent properties (e.g., high dielectric constant, heat resistance, and strong corrosion resistance), and promising applications [29,30]. Since the discovery of the gaseous yttrium monoxide (YO) molecule [31,32], theoretical studies have explored hypothetical YO phases [33], wherein Y assumes a +2 oxidation state. The unique $3d^1$ electronic configuration could induce metallization or magnetism in YO. Thus far, two bulk YO phases (e.g., *Pmna* and $P4/nmm$) have been theoretically proposed, however they have a high formation energy ($\Delta E_f = 44.67$ and $= 54.4$ meV/atom) with respect to decomposition into Y_2O_3 and Y [34], indicating that they are metastable.

Y is an intrinsic superconductor [22], and its compounds (e.g., $YBa_2Cu_3O_{7-x}$ [35]) are also superconducting. Moreover, theoretical calculations have predicted that a number of Y-containing phases (e.g., Y_2C_3 [36], YSH [37], YH_n ($n = 3,6,9,10$) [38–42]) are also superconducting. Simple TM oxides have drawn great attention because their elementary structures provide an ideal platform for studying valence states in TM atoms and exploring the origin of their properties. Thus far, several of them (e.g., LaO [43], NbO [44], and TiO [45]) have shown superconductivity. The highest T_c in simple TM oxides was measured to be ~5.5 K for TiO [45]. Taking these factors into consideration, it is conceivable that one could discover stable Y-O compounds with superconductivity and unique oxygenic motifs under high pressure.

In this work, we carry out extensive structure searches to uncover stable Y-O compounds via the particle swarm optimization algorithm [46,47]. In addition to finding the known Y-O compounds, four hitherto unknown phases (e.g., YO, YO_2, Y_2O_5, and YO_3) have been identified. The two stable YO structures (NaCl- and CsCl-type) are metallic, however, only the NaCl-type is superconducting, exhibiting the highest T_c value among the reported simple oxides. More intriguingly, our results show that the oxygen motifs present (e.g., O^{2-}, $O_2{}^{2-}$, or $O_2{}^{-}$) can be tuned by modulating the oxygen composition, playing a key role in the electronic properties of Y-O compounds. We hope our results will stimulate further investigations of O-rich TM compounds.

II. COMPUTATIONAL DETAILS

The reliable determination of the ground state structure of each chemical composition considered is the premise of determining phase stability, and subsequent study of the properties of select phases. A number of techniques have been proposed towards the computational determination of the global and important local minima of crystals given only the chemical composition, playing a leading role in the discovery of new materials [48,49]. Here, we employ a swarm-intelligence based structure search method, CALYPSO [46,47], which has been applied towards a plethora of materials from elemental solids to binary and ternary compounds [50–53]. We have performed extensive structure searches on the Y-O system with various Y_xO_y ($x = 1$, $y = 1$–6; $x = 2$, $y = 1$, 3, 5 and $x = 3$, $y = 4$) chemical compositions at 0 K and selected pressures of 1 atm, 50, 100, 200, and 300 GPa. The cell size considered is up to four formula units for Y_xO_y ($x = 1$, $y = 1$–4; $x = 2$, $y = 1$, 3), and one and two formula units for the other compositions.

Structural relaxation and electronic structure calculations are performed using density-functional theory [54,55] within the generalized gradient approximation of Perdew-Burke-Ernzerhof (PBE) [56], as implemented in the Vienna *ab initio* simulation package (VASP) [57]. The cut-off energy employed is 800 eV, in combination with a Monkhorst-Pack scheme with a dense k-point grid spacing of $2\pi \times 0.03$ Å^{-1}, yielding an energy converged to less than 1 meV/atom. The electron-ion interaction is described by using the projector augmented-wave [58] with $4s^24p^65s^14d^2$ and $2s^22p^4$ treated as the valence electrons of Y and O atoms, respectively. To further test the reliability of the adopted pseudopotentials for Y and O, the equation of states for YO_3 are calculated using the full-potential linearized augmented plane-wave method as implemented in the WIEN2K code [59], and the results are compared with VASP.

The relative thermodynamic stability of different Y−O compounds with respect to elemental Y and O solids at each pressure is evaluated according to the equation: $\Delta H(Y_xO_y) = [H(Y_xO_y) - xH(Y) - yH(O)]/(x + y)$, where $H = U + PV$ is the enthalpy of each species per formula unit (f.u.). To verify dynamic stability, the phonon spectra are obtained using the supercell approach with the finite displacement method [60], as implemented in the PHONOPY code [61]. The electron localization function (ELF) is used to gauge the degree of electron localization [62]. The electron-phonon coupling of the stable compounds are calculated within the framework of linear response theory via the QUANTUM ESPRESSO package [63]. We have calculated the superconducting T_c as estimated from the McMillan-Allen-Dynes formula [64–66]:

$$T_c = \frac{\omega_{\log}}{1.2} \exp\left[-\frac{1.04(1+\lambda)}{\lambda - \mu^*(1+0.62\lambda)}\right].$$

The electron-phonon coupling constant, λ, and the logarithmic average phonon frequency, $\omega_{\log}$, are calculated from the Eliashberg spectral function for the electron-phonon interaction:

$$\alpha^2F(\omega) = \frac{1}{N(E_F)} \sum_{kq,v} |g_{k,k+q,v}|^2 \delta(\varepsilon_k)\delta(\varepsilon_{k+q})\delta(\omega - \omega_{q,v}),$$

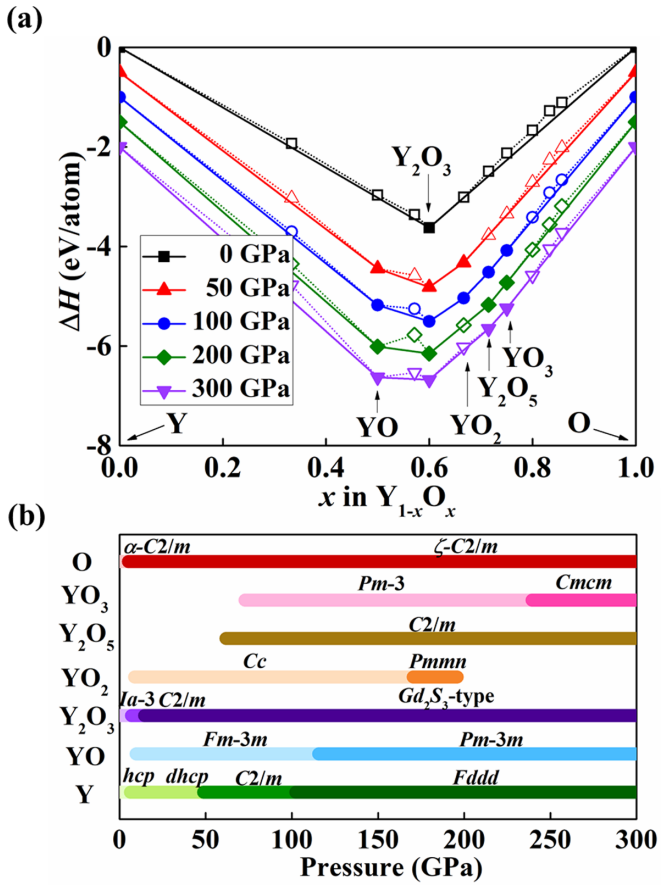

FIG. 1. (a) Phase stabilities of the Y-O compounds with respect to elemental Y and O_2 solids. The compounds sitting on the solid line (filled symbols) are thermodynamically stable, whereas the ones on the dotted lines (unfilled symbols) are metastable. The $P6_3/mmc$, $C2/m$, *and Fddd* phases for elemental Y solid [34,70,71], α and ζ phases of O_2 with $C2/m$ symmetry [72,73] are used to calculate the formation enthalpy per atom for each composition. (b) Pressure-composition phase diagram of the Y-O system in the range of 0–300 GPa.

where

$$\lambda = 2\int d\omega \frac{\alpha^2 F(\omega)}{\omega}; \omega_{\log} = \exp\left[\frac{2}{\lambda}\int \frac{d\omega}{\omega}\alpha^2 F(\omega)\ln(\omega)\right].$$

Herein, $N(E_F)$ is the electronic density of states at the Fermi level, $\omega_{q,v}$ is the phonon frequency of mode v at wave vector q, and $|g_{k,k+q,v}|$ is the electron-phonon matrix element between two electronic states with momenta k and $k+q$ at the Fermi level [67,68]. Further information about the structure searches and computational details can be found in the Supplemental Material [69].

III. RESULTS AND DISCUSSION

A. Phase stability of the Y-O system

The calculated convex hulls, which can be used to determine the relative stability of each composition, of the Y-O system at different pressures are presented in Fig. 1(a). The compounds lying on the convex hull, denoted by a solid line, are thermodynamically stable meaning they could potentially be synthesized given the correct conditions. The phases sitting on the dotted lines are either unstable or metastable (provided their phonons are real), and they will decompose into other Y_xO_y compounds or elemental Y and O solids if the kinetic barriers are not too high.

In the Y-O system, Y_2O_3 has the most negative ΔH at ambient conditions, and it sits on the convex hull in the whole pressure range. Its structural phase transitions under pressure have been extensively studied [74–77]. Thus far, four high-pressure phases (e.g., C-type with *Ia*-3, B-type with $C2/m$, A-type with P-$3m1$, and Gd_2S_3-type with *Pnma* symmetry) have been proposed to be stable between 0 and 60 GPa by experiment and theory. Here, we found that the cubic *Ia*-3 structure transforms to the monoclinic $C2/m$ phase at 6.8 GPa, and at 14.4 GPa to the orthorhombic *Pnma* structure, which remains thermodynamically stable until 300 GPa. Our results not only exclude the *A*-type candidate structure, but are also in agreement with recent experimental observations [74]. Moreover, the optimized crystal parameters are consistent with previous experiments and theory (Table S1). These results indicate that our adopted structure prediction method and computational method are suitable for the Y-O system.

With pressure, several new compounds (i.e., YO, YO_2, Y_2O_5, and YO_3) become thermodynamically stable. The calculated pressure-composition phase diagram of stable Y-O binary compounds is shown in Fig. 1(b), providing inspiration for experimental synthesis. Specifically, YO stabilizes in a NaCl-type structure with *Fm*-3*m* symmetry (*B*1) at 9.9 GPa, then transforms to a CsCl-type phase with *Pm*-3*m* symmetry (*B*2), and the phase transition sequence (e.g., $B1 \rightarrow B2$) is consistent with that of other simple metal oxides (i.e., CaO [78], TiO [18] and MgO [79]). Two proposed *Pnma* and *P*/4*nmm* YO phases [33] have lower enthalpy than the NaCl-type structure below ~5.5 GPa, but they are thermodynamically unstable with respect to Y_2O_3 plus Y (Figs. S2 and S3). The computed structural phase transition between *Cc* and *Pmmn* YO_2 is 170.3 GPa, and this stoichiometry is predicted to decompose into Y_2O_3 plus Y_2O_5 above 198.0 GPa. $C2/m$ Y_2O_5 is stable from 61.7 to 300 GPa. YO_3 becomes stabilized at 72.7 GPa within a cubic structure, and transforms into an orthorhombic phase with *Cmcm* symmetry at 239.3 GPa. Based on the calculated phonon dispersion curves, all of the predicted compounds are dynamically stable without any imaginary phonon modes in the whole Brillouin zone (Figs. S4 and S5).

B. Crystal structures

The most O-rich stoichiometry, YO_3, assumes a cubic structure [space group *Pm*-3, 2 f.u., Fig. 2(a)] above 72.7 GPa. The most striking structural feature is that all O atoms exist in quasimolecular O_2 units with an O−O distance of 1.48 Å at 100 GPa. This distance is slightly shorter than in a typical peroxide (O_2^{2-}) containing compound such as Li_2O_2, where they measure to be 1.55 Å at 1 atm [80]. Moreover, the calculated Bader partial charge is −0.70 for O, which is comparable to −0.86 in Li_2O_2 (Table S2). These results confirm this species can be viewed as an O_2^{2-} molecule wherein all of the atoms assume a -1 formal oxidation state. There are two kinds of Y atoms located at the vertex (Y1) and body center (Y2)

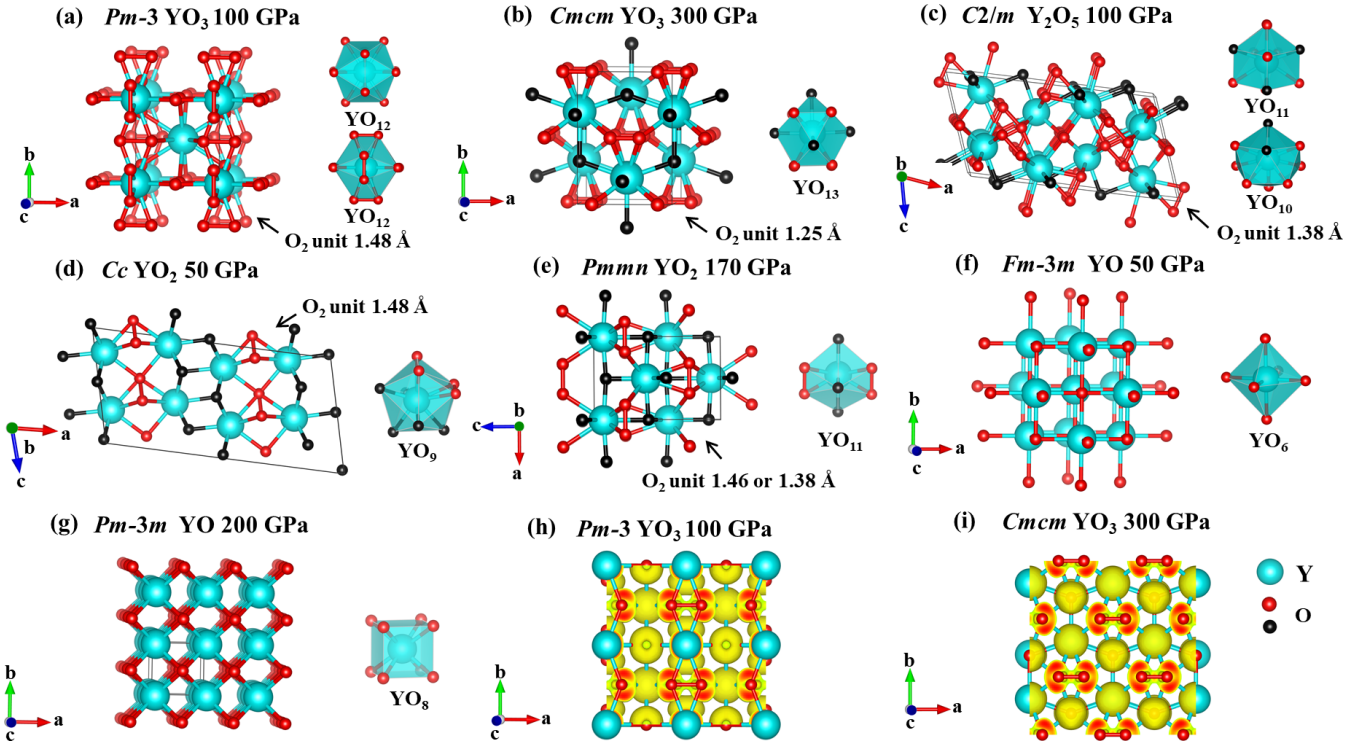

FIG. 2. Crystal structures of the predicted Y-O compounds and electron localization functions of two YO_3 phases. (a) *Pm*-3 YO_3 at 100 GPa, (b) *Cmcm* YO_3 at 300 GPa, (c) *C*2/*m* Y_2O_5 at 100 GPa, (d) YO_2 with *Cc* symmetry at 50 GPa, (e) Pmmn YO_2 at 170 GPa, (f) NaCl-type YO at 50 GPa, (g) CsCl-type YO at 200 GPa. In these structures, O atoms are represented by red and black spheres, and the blue spheres denote Y atoms. The calculated electron localization functions for (h) *Pm*-3 YO_3 and (i) *Cmcm* YO_3 with an isosurface of 0.6.

positions of the cubic lattice. They are 12-fold coordinated by O atoms, but the coordination polyhedra about them are different types of icosahedra [Fig. 2(a)]. Specifically, Y1 is coordinated by 12 O atoms within six O_2^{2-} units, whereas Y2 is coordinated by 12 O atoms coming from the 12 O_2^{2-}s. The Bader charges are 2.04 and 2.12 for Y1 and Y2 at 100 GPa, which is close to the value calculated for *Ia*-3 Y_2O_3 at 1 atm, 2.12 (Table S3), indicating that the oxidation state of Y in YO_3 is +3. Thus, the formula of the latter can be written as $Y^{3+}(O_2^{2-})_{1.5}$.

Upon further compression, *Pm*-3 YO_3 transforms into an orthorhombic structure [space group *Cmcm*, 4 f.u., Fig. 2(b)] above 239.3 GPa. This structure contains one Y atom sitting at the 4*c* position, and two inequivalent O atoms occupying the 4*c* and 8*e* sites. The first of these O atoms is coordinated by five Y atoms, whereas the later forms quasimolecular O_2 units that each surround four different Y atoms. Compared to *Pm*-3 YO_3, the O−O bond length (1.25 Å) in the quasimolecular O_2 units at 300 GPa is much shorter, and closer to the distance within the superoxide group (O^{2-}) in LiO_2 (NaO_2) at ambient pressure, 1.34 (1.35) Å. The resulting Bader charges are −1.1 and −0.42 for the two kinds of O atoms (Table S3), corresponding to O^{2-} and O_2^-. To the best of our knowledge, this is the first TM oxide containing O_2^- (superoxide) units.

Y_2O_5 stabilizes in a monoclinic structure [space group *C*2/*m*, 4 f.u., Fig. 2(c)] above 61.7 GPa, consisting of two inequivalent Y atoms. The first of these is tenfold and the second is 11-fold coordinated by O atoms, and both are enveloped within 16-faced coordination polyhedra. These high coordination numbers lead to the formation of quasimolecular O_2 units with an O−O distance of ∼1.38 Å at 100 GPa. According to the calculated Bader charges, each of the quasimolecular units corresponds to a peroxide (O_2^{2-}) anion, whereas the other O atoms exist in an O^{2-} form.

YO_2 assumes a monoclinic structure [space group *Cc*, 8 f.u., Fig. 2(d)], consisting of a ninefold coordinated face-sharing YO_9 distorted tetrakaidecahedron. From the nine O atoms, five are in the anionic form (O^{2-}), and the other four O atoms form two pairs of quasimolecular O_2 units with an O−O distance of 1.48 Å at 50 GPa. At higher pressures YO_2 transforms to an orthorhombic structure [space group *Pmmn*, 4 f.u., Fig. 2(e)], in which each Y atom is coordinated by 11 O atoms. As compared to *Cc* YO_2, *Pmmn* YO_2 is more densely packed, as can be seen in the variation of the pressure dependence of the *PV* and *U* terms (Fig. S6). Based on the O−O distance and Bader charge (Table S3), the two YO_2 phases also contain O^{2-} and O_2^{2-} motifs.

The long-pursued YO stoichiometry is predicted to be stable above 9.9 GPa in a NaCl-type structure [space group *Fm*-3*m*, 4 f.u. per cell, Fig. 2(f)]. With increasing pressure it transforms into a CsCl-type phase [space group *Pm*-3*m*, 1 f.u. per cell, Fig. 2(g)]. This is a first-order transition with an increase of coordination number from 6 to 8. Based on the Bader charge analysis, we can assign Y with a +2 formal oxidation state (Table S3). Detailed structural parameters of the stable Y-O compounds are provided in Table S4.

As mentioned above, the properties of oxides are closely related to the O motifs present in them (e.g., O^{2-}, O^{2-} and

O_2^{2-}, or their combinations). The coordination number in the predicted Y-O compounds gradually increases from 6 to 13 with increasing oxygen content. Meanwhile, the oxygen forms evolve from O^{2-} in YO and Y_2O_3, to the coexistence of O^{2-} and O_2^{2-} in YO_2 and Y_2O_5, to O_2^{2-} in *Pm*-3 YO_3, and to O^{2-} in *Cmcm* YO_3, indicating that the motifs present are correlated not only to the chemical composition but also to the crystal structures. Larger oxygen content in these phases promotes the formation of O_2^{2-} or O^{2-}. Because pressure is beneficial for stabilizing compounds with unusual stoichiometries [25], we hypothesize that under O-rich conditions pressure could be employed to synthesize these novel TM oxides.

C. Electronic properties

Inspired by the novel structures and presence of O^{2-}, O_2^{2-}, and O^{2-} in these predicted Y-O compounds, we have calculated their electronic band structures and projected density of states (PDOS) (Figs. S7 and S8) to explore the electronic properties and chemical bonding at the PBE level. In *Pm*-3 YO_3, there appears to be a large overlap between the Y 4*d* and O 2*p* states below the Fermi level [Fig. 3(a)], suggesting there may be charge transfer from Y to O, in agreement with the calculated Bader charges (Table S3) and ELF [Fig. 2(h)]. This phase is an indirect semiconductor with a band gap of 1.58 eV at 100 GPa. Its band gap increases with pressure [Fig. 3(c)], which is similar to BeO_2 [81], VO_4 [21], and Al_4O_7 [82], but different from BaO_2 [83]. Its semiconducting character is attributed to the presence of Y-O ionic bonding, and the covalently bonded O_2^{2-} motif, which is further confirmed by an analysis of the ELF [Fig. 2(i)]. The ELF between nearest neighbor O atoms is somewhat on the low side for a covalent bond, but it is similar to results obtained for FeO_2 [17]. *Cmcm* YO_3 is metallic, with the PDOS at the Fermi level arising mainly from the contribution of O 2p in O^{2-} [Fig. 3(d)], but it is nonmagnetic, similar to LiO_2 and NaO_2 (Fig. S9). This can be attributed to pressure-induced magnetic collapse [84]. The presence of localized electrons in O^{2-} indicates the formation of covalent bonding [Fig. 2(i)]. The predicted YO_2 and Y_2O_5 phases exhibit semiconducting character, and their PDOS distributions and chemical bonding are comparable to those of *Pm*-3 YO_3. As illustrated in Fig. S10, the ELF values between the closest neighboring O atoms in YO_2 and Y_2O_5 phases are similar to those in YO_3, showing covalent bonding character in the quasimolecular O_2 pairs. The band gap of Y_2O_5 increases with pressure [Fig. 3(c)], whereas the band gaps of the two YO_2 phases decrease (Fig. S11). The two YO phases (NaCl- and CsCl-type structure) are metallic, mainly originating from the contribution of Y 4*d* states [Figs. 3(e) and S8), which is in sharp contract with *Cmcm* YO_3. As mentioned above, Y in YO attains a +2 oxidation state, leaving an unoccupied d electron.

Motivated by the metallicity and high PDOS value at the Fermi level, we explored the potential superconductivity within *Cmcm* YO_3 and the two YO phases through the McMillan-Allen-Dynes formula with a typical choice of $\mu^* = 0.1$ [64–66,68,85]. The T_c value of *Cmcm*-YO_3 is 0 K at 300 GPa. For NaCl- and CsCl-type YO structures, only the NaCl-type is superconducting with a T_c of 13.0 K at 25 GPa,

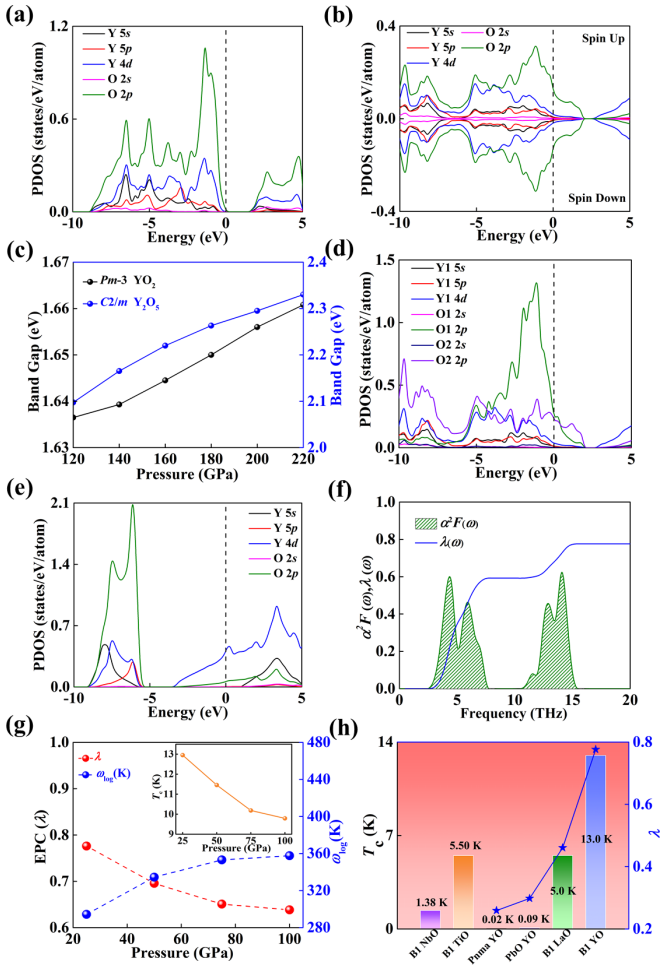

FIG. 3. (a) Projected density of states (PDOS) of *Pm*-3 YO_3 at 100 GPa. (b) Spin-dependent PDOS of YO_3 with *Cmcm* symmetry at 300 GPa. The complete symmetry of spin-up and spin-down PDOS indicates that YO_3 is nonmagnetic. (c) The band gap of *Pm*-3 YO_3 and Y_2O_5 as a function of pressure from 120 to 220 GPa at the PBE level. (d) PDOS of *Cmcm* YO_3 at 300 GPa. O1 corresponds to O^{2-}, and O2 atoms comprise the O_2^{2-} motifs. (e) PDOS of *Fm*-3*m* YO at 50 GPa. (f) The Eliashberg spectral function, $\alpha^2F(\omega)$, and integrated electron-phonon coupling parameter, $\lambda(\omega)$, of *Fm*-3*m* YO at 25 GPa. (g) The electron-phonon coupling coefficient λ (red dashed line) and the logarithmic average phonon frequency $\omega_{\log}$ (blue dashed line) as a function of pressure for YO. The critical temperature, T_c, (orange line) as a function of pressure is shown in the inset. (h) The T_c values of simple TM, TiO [45], and NbO [44], are obtained from the literature at ambient conditions. Other λ and T_c are calculated by using the same accuracy as used for *Fm-3m* YO (B1) at 25 GPa.

which is much higher than values reported for simple TM oxides (i.e., 1.38 K for NbO [44], 5.5 K for TiO [45], and 5 K for LaO [43]). The integrated electron-phonon coupling parameter, λ (ω), and Eliashberg spectral function, $\alpha^2F(\omega)$, are shown in Fig. 3(f). The calculated λ is 0.77, and the contribution of low-, mid-, and high-frequency modes to λ are 38.19% (below 7 THz), 3.72% (7 $\sim$ 11 THz), and 54.98% (above 11 THz), respectively. Therefore, the high-frequency phonon modes dominate superconductivity, similar to what has been found for the high-frequency H-derived vibrations

of high-T_c H_3S [6], LaH_{10} [42], and YH_{10} [40]. We also explored its pressure-dependant T_c. As shown in Fig. 3(g), T_c decreases with pressure (i.e., 10.2 K at 75 GPa and 9.8 K at 100 GPa), meanwhile λ decreases, and ω_{log} increases. The two metastable YO phases (*Pnma* and $P/4nmm$) are also superconducting, but possess rather low T_c values [Fig. 3(h)]. The high T_c value of NaCl-type YO is attributed to a strong electron-phonon coupling parameter λ [Fig. 3(h)] and high ω_{log} (Fig. S12) as compared with other TM oxides.

IV. CONCLUSIONS

To determine the structure of the long sought after bulk yttrium monoxide (YO) phase and explore potential O-rich Y-O compounds, we have predicted the crystal structures and phase stabilities of the Y-O system at high pressures by using first-principles swarm-intelligence structure search calculations. We conclude that YO stabilizes in a NaCl-type structure above 9.9 GPa, in which Y adopts a +2 formal oxidation state. Upon further compression, YO transforms to a CsCl-type structure. More interestingly, NaCl-type YO is superconducting with a critical temperature (T_c) of 13.0 K, becoming the compound with the highest T_c among the known TM monoxides. Moreover, three O-rich compounds (e.g., YO_2, Y_2O_5, and YO_3) are found to be stable at different pressures, exhibiting intriguing structural features like Y-centered polyhedra and quasimolecular O_2 units. More interestingly, the oxygen forms evolve from O^{2-}, to the coexistence of O^{2-} and O_2^{2-}, and to O^{2-} with increasing oxygen content in the stable Y-O compounds. YO_3 becomes an example of a TM superoxide. The identified Y-O compounds have rich electronic properties including semiconductivity, metallicity, and superconductivity. These finding not only deepen the understanding of TM oxides, but also stimulate future experimental and theoretical investigations.

ACKNOWLEDGMENTS

The authors acknowledge funding support from the Natural Science Foundation of China under Grants No. 21873017 and No. 21573037, the Postdoctoral Science Foundation of China under Grant No. 2013M541283, and the Natural Science Foundation of Jilin Province (20190201231JC). The work was carried out at National Supercomputer Center in Tianjin, and the calculations were performed on TianHe-1 (A). E.Z. acknowledges the NSF (DMR-1827815) for financial support.

[1] H.-K. Mao, X.-J. Chen, Y. Ding, B. Li, and L. Wang, Rev. Mod. Phys. **90**, 015007 (2018).
[2] J. A. Flores-Livas, L. Boeri, A. Sanna, G. Profeta, R. Arita, and M. Eremets, Phys. Rep. **856**, 1 (2020).
[3] E. Zurek and T. Bi, J. Chem. Phys. **150**, 50901 (2019).
[4] W. Cai, W. Lin, Y. Yan, K. P. Hilleke, J. Coles, J.-K. Bao, J. Xu, D. Zhang, D. Y. Chung, M. G. Kanatzidis, E. Zurek, and S. Deemyad, Chem. Mater. **32**, 6237 (2020).
[5] M. Somayazulu, M. Ahart, A. K. Mishra, Z. M. Geballe, M. Baldini, Y. Meng, V. V Struzhkin, and R. J. Hemley, Phys. Rev. Lett. **122**, 027001 (2019).
[6] A. P. Drozdov, M. I. Eremets, I. A. Troyan, V. Ksenofontov, and S. I. Shylin, Nature (London) **525**, 73 (2015).
[7] E. Snider, N. Dasenbrock-Gammon, R. McBride, M. Debessai, H. Vindana, K. Vencatasamy, K. V Lawler, A. Salamat, and R. P. Dias, Nature (London) **586**, 373 (2020).
[8] C. J. Pickard, I. Errea, and M. I. Eremets, Annu. Rev. Condens. Matter Phys. **11**, 57 (2020).
[9] S. Riedel and M. Kaupp, Coord. Chem. Rev. **253**, 606 (2009).
[10] Y. Quan, V. Pardo, and W. E. Pickett, Phys. Rev. Lett. **109**, 216401 (2012).
[11] W. Sun, Y. Song, X.-Q. Gong, L. Cao, and J. Yang, Chem. Sci. **6**, 4993 (2015).
[12] D. Luo, J. Lv, F. Peng, Y. Wang, G. Yang, M. Rahm, and Y. Ma, Chem. Sci. **10**, 2543 (2019).
[13] J. Lin, X. Du, M. Rahm, H. Yu, H. Xu, and G. Yang, Angew. Chemie Int. Ed. **59**, 9155 (2020).
[14] J. Lin, Z. Zhao, C. Liu, J. Zhang, X. Du, G. Yang, and Y. Ma, J. Am. Chem. Soc. **141**, 5409 (2019).
[15] D. W. Jeong, W. S. Choi, S. Okamoto, J. Kim, K. W. Kim, S. J. Moon, D. Cho, H. N. Lee, and T. W. Noh, Sci. Rep. **4**, 6124 (2014).
[16] G. Yang, Y. Wang, and Y. Ma, J. Phys. Chem. Lett. **5**, 2516 (2014).
[17] C. Lu, M. Amsler, and C. Chen, Phys. Rev. B **98**, 054102 (2018).
[18] X. Zhong, L. Yang, X. Qu, Y. Wang, J. Yang, and Y. Ma, Inorg. Chem. **57**, 3254 (2018).
[19] J. Zhang, A. R. Oganov, X. Li, K.-H. Xue, Z. Wang, and H. Dong, Phys. Rev. B **92**, 184104 (2015).
[20] J. Zhang, A. R. Oganov, X. Li, M. Mahdi Davari Esfahani, and H. Dong, J. Appl. Phys. **121**, 155104 (2017).
[21] X. Du, J. Zhang, H. Yu, J. Lin, S. Zhang, and G. Yang, Phys. Chem. Chem. Phys. **22**, 11460 (2020).
[22] L. Zhang, Y. Wang, J. Lv, and Y. Ma, Nat. Rev. Mater. **2**, 17005 (2017).
[23] M. A. ElGhazali, P. G. Naumov, Q. Mu, V. Süß, A. O. Baskakov, C. Felser, and S. A. Medvedev, Phys. Rev. B **100**, 014507 (2019).
[24] Z. Wang, H. Wang, J. S. Tse, T. Iitaka, and Y. Ma, Chem. Sci. **6**, 522 (2015).
[25] M. Miao, Y. Sun, E. Zurek, and H. Lin, Nat. Rev. Chem. **4**, 508 (2020).
[26] K. Yoshimatsu, O. Sakata, and A. Ohtomo, Sci. Rep. **7**, 12544 (2017).
[27] X. Zhong, M. Xu, L. Yang, X. Qu, L. Yang, M. Zhang, H. Liu, and Y. Ma, Npj Comput. Mater. **4**, 70 (2018).
[28] G. Adachi and N. Imanaka, Chem. Rev. **98**, 1479 (1998).
[29] A. Rosenflanz, M. Frey, B. Endres, T. Anderson, E. Richards, and C. Schardt, Nature (London) **430**, 761 (2004).
[30] J. Silver, M. I. Martinez-Rubio, T. G. Ireland, and R. Withnall, J. Phys. Chem. B **105**, 7200 (2001).
[31] R. J. Ackermann, E. G. Rauh, and R. J. Thorn, J. Chem. Phys. **40**, 883 (1964).
[32] J. M. Badie and B. Granier, Chem. Phys. Lett. **364**, 550 (2002).

[33] K. Z. Rushchanskii, S. Blügel, and M. Ležaić, Faraday Discuss. **213**, 321 (2019).

[34] F. H. Spedding, J. J. Hanak, and A. H. Daane, J. Less Common Met. **3**, 110 (1961).

[35] M. K. Wu, J. R. Ashburn, C. J. Torng, P. H. Hor, R. L. Meng, L. Gao, Z. J. Huang, Y. Q. Wang, and C. W. Chu, Phys. Rev. Lett. **58**, 908 (1987).

[36] X. Zhong, Y. Wang, F. Peng, H. Liu, H. Wang, and Y. Ma, Chem. Sci. **5**, 3936 (2014).

[37] J. Chen, W. Cui, J. Shi, M. Xu, J. Hao, A. P. Durajski, and Y. Li, ACS Omega **4**, 14317 (2019).

[38] D. Y. Kim, R. H. Scheicher, and R. Ahuja, Phys. Rev. Lett. **103**, 077002 (2009).

[39] K. Tanaka, J. S. Tse, and H. Liu, Phys. Rev. B **96**, 100502(R) (2017).

[40] F. Peng, Y. Sun, C. J. Pickard, R. J. Needs, Q. Wu, and Y. Ma, Phys. Rev. Lett. **119**, 107001 (2017).

[41] Y. Li, J. Hao, H. Liu, J. S. Tse, Y. Wang, and Y. Ma, Sci. Rep. **5**, 9948 (2015).

[42] H. Liu, I. I. Naumov, R. Hoffmann, N. W. Ashcroft, and R. J. Hemley, Proc. Natl. Acad. Sci. **114**, 6990 (2017).

[43] K. Kaminaga, D. Oka, T. Hasegawa, and T. Fukumura, J. Am. Chem. Soc. **140**, 6754 (2018).

[44] J. K. Hulm, C. K. Jones, R. A. Hein, and J. W. Gibson, J. Low Temp. Phys. **7**, 291 (1972).

[45] D. Wang, C. Huang, J. He, X. Che, H. Zhang, and F. Huang, ACS Omega **2**, 1036 (2017).

[46] Y. Wang, J. Lv, L. Zhu, and Y. Ma, Comput. Phys. Commun. **183**, 2063 (2012).

[47] Y. Wang, J. Lv, L. Zhu, and Y. Ma, Phys. Rev. B **82**, 094116 (2010).

[48] Z. Falls, P. Avery, X. Wang, K. P. Hilleke, and E. Zurek, J. Phys. Chem. C (2020).

[49] E. Zurek, in *Reviews in Computational Chemistry*, Vol. 29 (Wiley, New York, 2016), Chap. 5, pp. 274–326.

[50] J. Lv, Y. Wang, L. Zhu, and Y. Ma, Phys. Rev. Lett. **106**, 015503 (2011).

[51] M. Miao, Nat. Chem. **5**, 846 (2013).

[52] L. Zhu, H. Liu, C. J. Pickard, G. Zou, and Y. Ma, Nat. Chem. **6**, 644 (2014).

[53] H. Wang, J. S. Tse, K. Tanaka, T. Iitaka, and Y. Ma, Proc. Natl. Acad. Sci. U. S. A. **109**, 6463 (2012).

[54] W. Kohn and L. J. Sham, Phys. Rev. **140**, A1133 (1965).

[55] P. Hohenberg and W. Kohn, Phys. Rev. **136**, B864 (1964).

[56] J. P. Perdew, K. Burke, and M. Ernzerhof, Phys. Rev. Lett. **80**, 891 (1998).

[57] G. Kresse and J. Furthmüller, Phys. Rev. B **54**, 11169 (1996).

[58] J. J. Mortensen, L. B. Hansen, and K. W. Jacobsen, Phys. Rev. B **71**, 035109 (2005).

[59] P. Blaha, K. Schwarz, P. Sorantin, and S. B. Trickey, Comput. Phys. Commun. **59**, 399 (1990).

[60] K. Parlinski, Z. Q. Li, and Y. Kawazoe, Phys. Rev. Lett. **78**, 4063 (1997).

[61] A. Togo, F. Oba, and I. Tanaka, Phys. Rev. B **78**, 134106 (2008).

[62] A. D. Becke and K. E. Edgecombe, J. Chem. Phys. **92**, 5397 (1990).

[63] P. Giannozzi, S. Baroni, N. Bonini, M. Calandra, R. Car, C. Cavazzoni, D. Ceresoli, G. L. Chiarotti, M. Cococcioni, I. Dabo, A. Dal Corso, S. de Gironcoli, S. Fabris, G. Fratesi, R. Gebauer, U. Gerstmann, C. Gougoussis, A. Kokalj, M. Lazzeri, L. Martin-Samos, N. Marzari, F. Mauri, R. Mazzarello, S. Paolini, A. Pasquarello, L. Paulatto, C. Sbraccia, S. Scandolo, G. Sclauzero, A. P. Seitsonen, A. Smogunov, P. Umari, and R. M. Wentzcovitch, J. Phys.: Condens. Matter **21**, 395502 (2009).

[64] L. N. Oliveira, E. K. U. Gross, and W. Kohn, Phys. Rev. Lett. **60**, 2430 (1988).

[65] M. Lüders, M. A. L. Marques, N. N. Lathiotakis, A. Floris, G. Profeta, L. Fast, A. Continenza, S. Massidda, and E. K. U. Gross, Phys. Rev. B **72**, 024545 (2005).

[66] P. B. Allen and R. C. Dynes, Phys. Rev. B **12**, 905 (1975).

[67] P. B. Allen and B. Mitrović, in *Solid State Physics*, edited by H. Ehrenreich, F. Seitz, and D. Turnbull (Academic Press, New York, 1983), pp. 1–92.

[68] J. P. Carbotte, Rev. Mod. Phys. **62**, 1027 (1990).

[69] See Supplemental Material at http://link.aps.org/supplemental/10.1103/PhysRevMaterials.5.044802 for computational details.

[70] G. K. Samudrala, G. M. Tsoi, and Y. K. Vohra, J. Phys.: Condens. Matter **24**, 362201 (2012).

[71] P. Li, T. Mei, Z. Lu, L. Xiang, X. Zhang, X. Du, J. Wang, and H. Chen, Comput. Mater. Sci. **159**, 428 (2019).

[72] C. S. Barrett, L. Meyer, and J. Wasserman, J. Chem. Phys. **47**, 592 (1967).

[73] Y. Ma, A. R. Oganov, and C. W. Glass, Phys. Rev. B **76**, 064101 (2007).

[74] H. Yusa, T. Tsuchiya, N. Sata, and Y. Ohishi, Inorg. Chem. **49**, 4478 (2010).

[75] K. Umemoto and R. M. Wentzcovitch, Phys. Chem. Miner. **38**, 387 (2011).

[76] X. Li, X. Xia, H. Xu, S. Zhong, and D. He, Mater. Lett. **239**, 82 (2019).

[77] I. Halevy, R. Carmon, M. L. Winterrose, O. Yeheskel, E. Tiferet, and S. Ghose, J. Phys. Conf. Ser. **215**, 12003 (2010).

[78] N. Hammou, A. Zaoui, and M. Ferhat, J. Alloys Compd. **815**, 152424 (2020).

[79] Q. Zhu, A. R. Oganov, and A. O. Lyakhov, Phys. Chem. Chem. Phys. **15**, 7696 (2013).

[80] L. G. Cota and P. de la Mora, Acta Crystallogr. Sect. B **61**, 133 (2005).

[81] S. Zhang, F. Li, H. Xu, and G. Yang, Inorg. Chem. **56**, 5233 (2017).

[82] Y. Liu, A. R. Oganov, S. Wang, Q. Zhu, X. Dong, and G. Kresse, Sci. Rep. **5**, 9518 (2015).

[83] G. F. Carter and D. H. Templeton, J. Am. Chem. Soc. **75**, 5247 (1953).

[84] M. B. Maple, J. Wittig, and K. S. Kim, Phys. Rev. Lett. **23**, 1375 (1969).

[85] W. L. McMillan, Phys. Rev. **167**, 331 (1968).